Improved Expressions for Calculating the Impedance of Differential Feed Rectangular Microstrip Patch Antennas

Ziqiang Tong, *Student Member, IEEE*, Andreas Stelzer, *Member, IEEE*, and Wolfgang Menzel, *Fellow, IEEE*

***Abstract*—This letter presents an analysis of the impedances of differential feed microstrip rectangular patch antennas. It is shown that the impedance of a differential feed antenna exhibits cosine squared behavior over the feed distance. We present improved expressions for calculating the impedance match feed positions of a differential feed rectangular microstrip patch antenna with given dimensions, on the base of which we designed two antenna prototypes. Both simulation and measurement results match our theoretical prediction.**

***Index Terms*—Cavity model, differential feed microstrip patch antenna, impedance match.**

I. Introduction

DIFFERENTIAL feed microstrip patch antennas (DMPAs) are becoming increasingly popular due to their compact integration with fully differential monolithic microwave integrated circuits (MMICs) and their good radiation performance, etc. Various designs of differential feed antennas have been reported in the last decade [1]–[3]. However, further analysis for the antenna impedance with differential feed is still an issue, e.g., the calculation of impedance matched points for differentially-driven patch antenna, etc.

The cavity model has been used successfully to analyze and to provide physical insight into the single-ended feed microstrip patch antenna (SMPA) [4]. A quantitative analysis of the antenna impedance of DMPAs is shown in [3]. In this letter, we extend the analysis to reveal the relationship of antenna impedance with two different feed mechanisms. Furthermore, we provide concise expressions of calculating the impedance matched feed points of rectangular patch antenna by a differential feed. Two antennas of different substrate thickness (t) were designed using this theory. Both simulation and prototype measurement results are in accordance with our theoretical predictions.

Manuscript received April 27, 2012; revised July 19, 2012 accepted July 25, 2012. Date of publication August 20, 2012; date of current version August 30, 2012. This work was supported by the Austrian Center of Competence in Mechatronics (ACCM).

Z. Tong is with the Institute for Communications Engineering and RF-Systems, Johannes Kepler University Linz, Linz 4040, Austria (e-mail: z.tong@nthfs.jku.at).

A. Stelzer is with the Institute for Communications Engineering and RF-Systems and the Christian Doppler Laboratory for Integrated Radar Sensors, Johannes Kepler University Linz, Linz 4040, Austria (e-mail: a.stelzer@nthfs.jku.at).

W. Menzel is with the Institute of Microwave Techniques, University of Ulm, Ulm 89081, Germany (email: wolfgang.menzel@uni-ulm.de).

Color versions of one or more of the figures in this paper are available online at http://ieeexplore.ieee.org.

Digital Object Identifier 10.1109/LMWC.2012.2212240

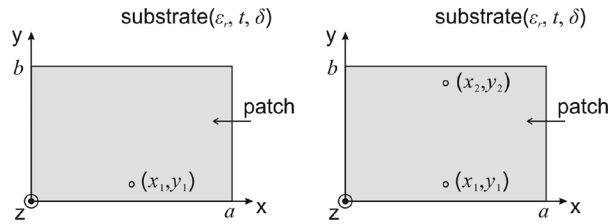

Fig. 1. Rectangular microstrip patch with single-ended feed (a) and differential feed (b).

II. Impedance Analysis

Fig. 1 shows rectangular microstrip patch antennas with different feed mechanisms. The feed point of the single-ended feed antenna [Fig. 1(a)] is at (x_1, y_1). The differential feed antenna [Fig. 1(b)] has two feed points, (x_1, y_1) and (x_2, y_2), respectively.

First, let us recapitulate (5) in [4] for antenna impedance with single-ended feed

$$Z_s = j\omega\mu_0 t \sum_{m,n=0}^{\infty} \frac{\phi_{mn}^2(x_1,y_1) j_0^2\left(\frac{m\pi d_e}{2a_e}\right)}{k_{mn}^2 - k_e^2} \tag{1}$$

where ω is the angular frequency, μ_0 is the permeability of vacuum. Since the patch exhibits fringing effects, the physical dimensions of the patch (a, b) are replaced with the effective dimensions (a_e, b_e)

$$\phi_{mn}(x,y) = \sqrt{\frac{\varepsilon_{0m}\varepsilon_{0n}}{a_e b_e}} \cos\left(\frac{m\pi x}{a_e}\right) \cos\left(\frac{n\pi y}{b_e}\right) \tag{1a}$$

$$k_{mn}^2 = \left(\frac{m\pi}{a_e}\right)^2 + \left(\frac{n\pi}{b_e}\right)^2 \tag{1b}$$

$$k_e^2 = \varepsilon_r(1 - j\delta_e)k_0^2 \tag{1c}$$

$$j_0(x) = \frac{\sin(x)}{x} \tag{1d}$$

where k_0 is the wavenumber, and ε_r is the relative permittivity. The definitions of the remaining parameters $(\varepsilon_{0m}, \delta_e, d_e)$ can be found in [4]. The subscript s of Z_s denotes a single-ended feed. The subscript (m, n) indicates the mode indices in the x and y axis. Typically, x_1 is selected as $a_e/2$, and y_1 represents feed distance measured from the edge of the patch to the feed point.

The sum for Z_s in (1) can be rewritten as

$$Z_s = \sum_{m,n=0}^{\infty} Z_{s,mn} \tag{2}$$

where

$$Z_{s,mn} = j\omega\mu_0 t \frac{\phi_{mn}^2(x_1,y_1) j_0^2\left(\frac{m\pi d_e}{2a_e}\right)}{k_{mn}^2 - k_e^2}. \tag{2a}$$

$Z_{s,mn}$ represents the antenna impedance of the TM_{mn} mode and is called mode impedance here. Compared to [(1a)-(1d)], for a fixed mode number (m,n), $\mathrm{Re}[j/(k_{mn}^2-k_e^2)]$ reaches a maximum value when $k_{mn}^2=\varepsilon_r k_0^2$. Therefore, the peak value of $\mathrm{Re}[Z_{s,mn}]$ occurs at its resonant frequency (f_{mn}), and drops quickly away from the resonant frequency. In another word, the value of $\mathrm{Re}[Z_s]$ around the fundamental resonant frequency (f_{01}) is dominated by the value of $\mathrm{Re}[Z_{s,01}]$.

The resonant resistance R_s is defined as $\mathrm{Re}[Z_s]$ at f_{01}, and it can be calculated as

$$R_s(y=y_1)=\mathrm{Re}[Z_s]_{f_{01}}\approx\mathrm{Re}[Z_{s,01}]_{f_{01}}\propto\cos^2\left(\frac{\pi y_1}{b_e}\right). \quad (3)$$

Comparing (1.a) with (3), we obtain the following relationship for $R_s(y=y_1)$ over the feed distance (y_1):

$$R_s(y=y_1)=R_s(y=0)\cos^2\left(\frac{\pi y_1}{b_e}\right) \quad (4)$$

where $R_s(y=0)$ represents the antenna impedance with the feed point at the edge of the patch [6]. It shows that the impedance of a patch antenna with single-ended feed exhibits a cosine squared behavior over the feed distance.

Next, we address the antenna impedance with a differential feed. It may be calculated using the Z parameters [3]

$$Z_d=\frac{V_d}{I}=2(Z_{11}-Z_{12})=2(Z_{22}-Z_{21}) \quad (5)$$

where

$$Z_{11}=j\omega\mu_0 t\sum_{m,n=0}^{\infty}\frac{\phi_{mn}^2(x_1,y_1)j_0^2\left(\frac{m\pi d_e}{2a_e}\right)}{k_{mn}^2-k_e^2} \quad (5a)$$

$$Z_{12}=j\omega\mu_0 t\sum_{m,n=0}^{\infty}\frac{\phi_{mn}(x_1,y_1)\phi_{mn}(x_2,y_2)j_0^2\left(\frac{m\pi d_e}{2a_e}\right)}{k_{mn}^2-k_e^2}. \quad (5b)$$

The subscript d of Z_d denotes a differential feed. Z_{11} and Z_{12} are called self impedance and mutual impedance respectively. Compared to (5a) and (5b) to (1), we can find Z_{11} is same as Z_s, while Z_{12} is different. Now we compare Z_{12} with Z_{11}.

Similar as Z_s, we introduce mode impedance $Z_{d,mn}$ for Z_d

$$Z_d=\sum_{m,n=0}^{\infty}Z_{d,mn}=2\sum_{m,n=0}^{\infty}(Z_{11,mn}-Z_{12,mn}) \quad (6)$$

where

$$Z_{11,mn}=j\omega\mu_0 t\frac{\phi_{mn}^2(x_1,y_1)j_0^2\left(\frac{m\pi d_e}{2a_e}\right)}{k_{mn}^2-k_e^2} \quad (6a)$$

$$Z_{12,mn}=j\omega\mu_0 t\frac{\phi_{mn}(x_1,y_1)\phi_{mn}(x_2,y_2)j_0^2\left(\frac{m\pi d_e}{2a_e}\right)}{k_{mn}^2-k_e^2}. \quad (6b)$$

Obviously, the self-mode-impedance, $Z_{11,mn}$, is equal to $Z_{s,mn}$ in (2a). It is related to the mutual-mode-impedance, $Z_{12,mn}$, as follows:

$$\frac{Z_{11,mn}}{Z_{12,mn}}=\frac{\phi_{mn}(x_1,y_1)}{\phi_{mn}(x_2,y_2)}=\frac{\cos\left(\frac{m\pi x_1}{a_e}\right)\cos\left(\frac{n\pi y_1}{b_e}\right)}{\cos\left(\frac{m\pi x_2}{a_e}\right)\cos\left(\frac{n\pi y_2}{b_e}\right)}. \quad (7)$$

For the typical feed positions, $x_1=x_2=a_e/2$, and $y_1=b_e-y_2$, we can obtain

$$\frac{Z_{11,mn}}{Z_{12,mn}}=\frac{\cos\left(\frac{n\pi y_1}{b_e}\right)}{\cos\left(\frac{n\pi(b_e-y_1)}{b_e}\right)}=\begin{cases}1, & n=even\\ -1, & n=odd\end{cases}. \quad (8)$$

Inserting (8) into (6) results in

$$Z_d=\sum_{m,n=0}^{\infty}Z_{d,mn}=4\sum_{m=0,n=2i+1}^{\infty}Z_{11,mn}=4\sum_{m=0,n=2i+1}^{\infty}Z_{s,mn}. \quad (9)$$

Up to this point, we have built the relationship between Z_d and Z_s using the mode impedance $Z_{11,mn}(Z_{s,mn})$. Equation (9) implies that $Z_{d,mn}$ is zero if the mode index n is even, while $Z_{d,mn}$ is four times $Z_{s,mn}$ if n is odd. The fundamental mode of the antenna is TM_{01}, and the next two higher order modes are TM_{20} and TM_{21}. Here we assume that $1.5b_e>a_e>b_e$. Therefore, $Z_{d,20}$ and $Z_{d,21}$ are zero, while $Z_{d,01}$ is four times $Z_{s,01}$.

Similar as R_s, we define the resonant resistance R_d as $\mathrm{Re}[Z_d]$ at f_{01}. The assumption of (3) is still valid. Therefore, we calculate R_d as follows:

$$R_d(y=y_1)\approx R_{d,01}=4R_{s,01}\propto\cos^2\left(\frac{\pi y_1}{b_e}\right). \quad (10)$$

Equation (10) implies some interesting results:

First, the resonant resistance of the antenna with differential feed exhibits cosine squared behavior over the feed distance, which is the same as that for a single-ended feed antenna

$$R_d(y=y_1)=R_d(y=0)\cos^2\left(\frac{\pi y_1}{b_e}\right) \quad (11)$$

where $R_d(y=0)$ represents the antenna impedance with differential feed points at the edges of patch.

Secondly, the impedance match position for the antenna with differential feed can be calculated from R_s:

$$R_d(y=y_1)\approx 4R_s(y=y_1)=4R_s(y=0)\cos^2\left(\frac{\pi y_1}{b_e}\right). \quad (12)$$

Equation (12) shows that the resonant resistance of the differential feed antenna is four times that of the single-ended feed antenna for the same feed distance (y_1). This can be verified by the results shown in [3, Fig. 9-11]. It is worth to note that the resonant resistances (R_d) disappear when two feed positions are too close [7].

Usually, the reference impedance of the differential feed antenna is selected as 100 Ω, which is twice the single-ended feed antenna. Thus, the impedance matched feed distance of the differential feed antenna ($y_{d,100\ \Omega}$) and that of the single-ended feed antenna ($y_{s,50\ \Omega}$) are related by comparing (4) and (12)

$$\cos\left(\frac{\pi y_{d,100\ \Omega}}{b_e}\right)=\frac{\cos\left(\frac{\pi y_{s,50\ \Omega}}{b_e}\right)}{\sqrt{2}}. \quad (13)$$

If we normalize the feed distance y by $\tilde{y}=y/b_e$, (13) can be

$$\cos(\pi\tilde{y}_{d,100\ \Omega})=\frac{\cos(\pi\tilde{y}_{s,50\ \Omega})}{\sqrt{2}}. \quad (14)$$

Obviously, the normalized feed distance of the DMPA ($\tilde{y}_{d,100\ \Omega}$) is larger than that of the SMPA ($\tilde{y}_{s,50\ \Omega}$). That means

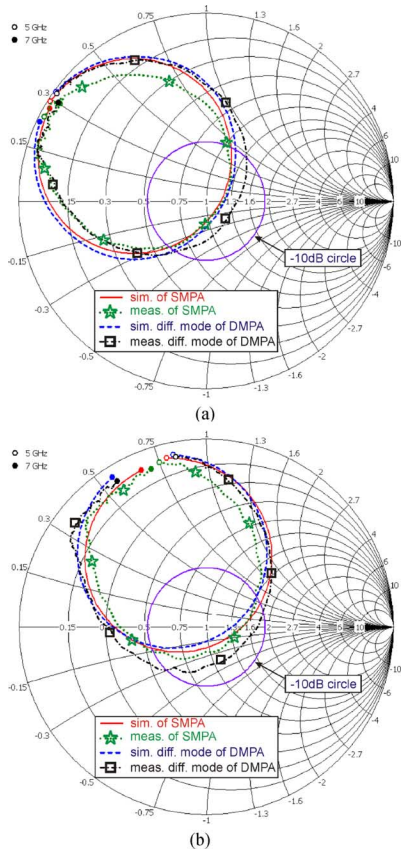

Fig. 2. Simulation and measurement of reflection coefficients (S_{11}) of SMPA and DMPA for substrate thickness $t_1 = 0.0762$ cm, $y_{s,50\ \Omega} = 0.6350$ cm, $y_{d,100\ \Omega} = 0.7270$ cm, $2\Delta b = 0.1333$ cm (a) and $t_2 = 0.1588$ cm, $y_{s,50\ \Omega} = 0.6799$ cm, $y_{d,100\ \Omega} = 0.7921$ cm, $2\Delta b = 0.2404$ cm (b).

the impedance match feed point of differential antenna is more close to the patch center compared to that of the single-ended antenna. This also explains the behaviors of the shorted-end quarter-wave patch antenna [5], which has similar E-field distribution of half of the differential feed patch antenna.

III. Prototype Test

In order to validate our theoretical expressions, we designed two groups of test antennas for two different feed mechanisms. Taconic TLY-5 ($\varepsilon_r = 2.2$) with two different thicknesses ($t_1 = 0.0762$ cm, $t_2 = 0.1588$ cm) was selected as the substrate material. Patches with identical dimensions ($a = 1.9$ cm, $b = 1.6$ cm) were used as radiating element for both thicknesses. The reference impedances of single-ended feed and differential feed antennas were selected as 50 Ω and 100 Ω respectively.

The calculated feed distances of the SMPA and the DMPA are listed in the caption of Fig. 2. It is worth to emphasize that the results calculated from (4) and (11) are effective feed distances, which are the distances from the effective edges of the patch to the feed points. The physical feed distances (measured from the physical edge of the patch) are $y_{s,50\ \Omega} - \Delta b$ and $y_{d,100\ \Omega} - \Delta b$ respectively, where Δb is the fringing effects extension [8].

Both antennas with probe feed were constructed and simulated using the 3-D EM simulation tools CST MWS. The simulation models are the same as models in Fig. 1. The simulated S_{11} of single-ended feed and differential feed antennas, which are normalized to 50 Ω and 100 Ω respectively, are shown in Fig. 2. It shows that given proper selection of feed positions, antenna patches with different feed mechanisms are excited in the same fundamental resonant mode and thus exhibit the same frequency behaviors.

The prototype antennas were fabricated and measured. The differential antennas were measured as two-port devices and the reflection coefficients were calculated by mode conversion matrix [9]. The measured and simulated S_{11} are plotted in Fig. 2. They match very well, confirming the validity of our theoretical expressions.

IV. Conclusion

We have presented a quantitative analysis of the impedance of patch antennas with differential feed. We have shown that the antenna impedance with differential feed exhibits the cosine-squared behavior over the feed distance. Using mode impedances, we found a relationship between the impedances of the antennas with two different feed mechanisms. For the same antenna feed distance, the antenna impedance of a differential feed antenna around the fundamental resonant frequency is four times that of a single-ended feed antenna. We have presented simple expressions for calculating the impedance match feed position of a rectangular patch antenna with differential feed which we used to design two antenna prototypes. Simulations and measurements results verify the validity of our theoretical expressions.

Acknowledgment

The authors would like to thank R. Rudersdorfer, Johannes Kepler University, Linz, for his assistance in the manufacturing process.

References

[1] Z. N. Chen and M. Y. W. Chia, "A novel center-slot-fed suspended plate antenna," *IEEE Trans. Antennas Propag.*, vol. 51, no. 6, pp. 1407–1410, Jun. 2003.

[2] Q. Xue, X. Y. Zhang, and C. K. Chin, "A novel differential-fed patch antenna," *IEEE Antennas Wireless Propag. Lett.*, vol. 5, pp. 471–474, Dec. 2006.

[3] Y. P. Zhang and J. J. Wang, "Theory and analysis of differentially-driven microstrip antennas," *IEEE Trans. Antennas Propag.*, vol. 54, no. 4, pp. 1092–1099, Apr. 2006.

[4] W. F. Richards, Y. T. Lo, and D. D. Harrison, "An improved theory for microstrip antennas and applications," *IEEE Trans. Antennas Propag.*, vol. AP-29, no. 1, pp. 38–46, Jan. 1981.

[5] K. F. Lee, Y. X. Guo, J. A. Hawkins, R. Chair, and K. M. Luk, "Theory and experiment on microstrip patch antenna with shorting walls," *Proc. Inst. Elect. Eng.*, vol. 147, no. 6, pp. 521–525, 2000.

[6] A. G. Derneryd, "Theoretical investigation of the rectangular microstrip antenna element," *IEEE Trans. Antennas Propag.*, vol. AP-26, no. 4, pp. 532–535, Jul. 1978.

[7] Y. P. Zhang, "Electrical separation and fundamental resonance of differentially-driven microstrip antennas," *IEEE Trans. Antennas Propag.*, vol. 59, no. 4, pp. 1078–1084, Apr. 2011.

[8] J. R. James, P. S. Hall, and C. Wood, *Microstrip Antenna: Theoryand Design*. London, U.K.: Peter Peregrinus Ltd, 1981, ch. 4.

[9] D. Bockelman and W. Eisenstadt, "Combined differential and common-mode scattering parameters: Theory and simulation," *IEEE Trans. Microw. Theory Tech.*, vol. 43, no. 7, pp. 1530–1539, Jul. 1995.